HHS Public Access

Author manuscript

Cell Rep. Author manuscript; available in PMC 2018 January 19.

Published in final edited form as:

Cell Rep. 2017 October 31; 21(5): 1304–1316. doi:10.1016/j.celrep.2017.10.026.

Evolutionarily conserved roles for blood-brain barrier xenobiotic transporters in endogenous steroid partitioning and behavior

Samantha J. Hindle[1,¶], **Roeben N. Munji**[1,2,3,4,¶], **Elena Dolghih**[5], **Garrett Gaskins**[5,6,7], **Souvinh Orng**[1], **Hiroshi Ishimoto**[8], **Allison Soung**[3,4], **Michael DeSalvo**[1], **Toshihiro Kitamoto**[9], **Michael J. Keiser**[5,6,7], **Matthew P. Jacobson**[5], **Richard Daneman**[3,4,*], and **Roland J. Bainton**[1,*,$]

[1]Department of Anesthesia and Perioperative Care, University of California San Francisco, San Francisco, CA, USA

[2]Division of Clinical Pharmacology and Experimental Therapeutics, University of California San Francisco, San Francisco, CA, USA

[3]Department of Anatomy, University of California San Francisco, San Francisco, CA, USA

[4]Department of Pharmacology, University of California San Diego, La Jolla, CA, USA

[5]Department of Pharmaceutical Chemistry, University of California San Francisco, San Francisco, CA, USA

[6]Institute for Neurodegenerative Disease, University of California San Francisco, San Francisco, CA, USA

[7]Department of Bioengineering and Therapeutic Sciences, University of California San Francisco, San Francisco, CA, USA

[8]Division of Biological Science, Graduate School of Science, Nagoya University, Japan

[9]Department of Anesthesia, University of Iowa, Iowa City, Iowa, USA

Summary

CNS chemical protection depends upon discrete control of small-molecule access by the blood-brain barrier (BBB). Curiously, some drugs cause CNS side effects despite negligible transit past the BBB. To investigate this phenomenon, we asked whether the highly BBB-enriched drug efflux

*Correspondence: Dr. Roland J. Bainton, Department of Anesthesia and Perioperative Care, University of California San Francisco, 600 16th Street, S312C Genentech Hall, San Francisco, CA, 91518, USA. roland.bainton@ucsf.edu; Dr. Richard Daneman, Department of Pharmacology, University of California San Diego, 9500 Gilman drive, Box 0636, La Jolla, CA, 92093 USA. rdaneman@ucsd.edu.

$Lead contact

¶Authors contributed equally

Author contributions

Experiments were conceived by S.J.H., R.N.M., E.D., G.G., H.I., T.K., M.J.K., M.P.J., R.D., and R.J.B. Experiments were performed by S.J.H., R.N.M., E.D., G.G., S.O., H.I., A.S., and M.D. Data were analyzed by S.J.H., R.N.M., E.D., G.G., H.I., M.J.K., and A.S. Manuscript was written by S.J.H., R.N.M., E.D., G.G., H.I., T.K., M.J.K., M.P.J., R.D., and R.J.B.

transporter Mdr1 has dual functions in controlling drug and endogenous molecule CNS homeostasis. If this is true, then brain-impermeable drugs could induce behavioral changes by affecting brain levels of endogenous molecules. Using computational, genetic and pharmacologic approaches across diverse organisms we demonstrate that BBB-localized efflux transporters are critical for regulating brain levels of endogenous steroids, and steroid-regulated behaviors (sleep in *Drosophila* and anxiety in mice). Furthermore, we show that Mdr1-interacting drugs are associated with anxiety-related behaviors in humans. We propose a general mechanism for common behavioral side effects of prescription drugs: pharmacologically challenging BBB efflux transporters disrupts brain levels of endogenous substrates, and implicates the BBB in behavioral regulation.

ETOC BLURB

Hindle *et al.* shed light on the curious finding that some drugs cause behavioral side effects despite negligible access into the brain. These authors propose a unifying hypothesis that links Blood-Brain Barrier drug transporter function and brain access of circulating steroids to common CNS adverse drug responses.

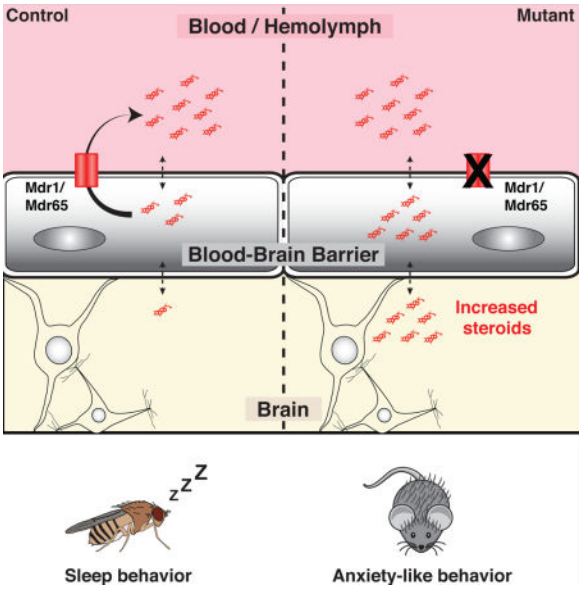

Introduction

The maintenance of central nervous system (CNS) function depends upon its regulated isolation from circulating drugs and toxins (xenobiotics), as well as endogenous molecules produced in the periphery. The importance of insulating neural tissue is evidenced by the conserved molecular and anatomic properties of blood-brain barriers (BBBs) (Fig. 1A). The vertebrate BBB is composed of brain vascular endothelial cells (BVECs), pericytes, basal lamina, and the endfeet of astrocytes. BVECs are specialized to protect the CNS as, compared to peripheral endothelial cells, they are enriched for tight junction components, chemoprotective ATP-Binding Cassette (ABC) drug efflux transporters and nutrient influx transporters (Daneman et al., 2010, Daneman, 2012). Similar to vertebrate BVECs,

Drosophila melanogaster focuses chemoprotective physiology into a single functionally polarized cellular layer, the subperineurial glia (SPG). The SPG surround the CNS, separating it from the blood (hemolymph) (Stork et al., 2008), and possess the hallmark properties of the vertebrate BBB: tight barrier physiology, potent xenobiotic effluxers and nutrient influx transporters (Mayer et al., 2009, DeSalvo et al., 2014, Hindle and Bainton, 2014).

BVEC tight junctions physically isolate peripherally produced hydrophilic molecules, like catecholamines, from the CNS, allowing synaptic regulation that is independent from the peripheral nervous system (Tsukita et al., 2001). Small lipophilic molecules, however, are able to freely diffuse across the plasma membrane, requiring an active, ATP-driven chemical efflux transport barrier to limit their buildup in the brain. The BBB-enriched ABC Type B efflux transporter Mdr1 (P-glycoprotein/ABCB1) is known to contribute to this barrier (Loscher and Potschka, 2005b, van Asperen et al., 1996, Loscher and Potschka, 2005a).

Mdr1 is expressed at the BBB and peripherally, in sites such as gut, kidney and other endothelial cells (Thiebaut et al., 1987, Cordon-Cardo et al., 1989). Unlike most transporters, it has a very broad spectrum of substrates, including hundreds of drugs and endogenous molecules (Tsuruo et al., 1982a, Tsuruo et al., 1982b, Tsuruo et al., 1983, Naito et al., 1989, Silbermann et al., 1989, Ueda et al., 1992, Ford, 1996, Uhr et al., 2002, Muller et al., 2003, Schoenfelder et al., 2012). Indeed, acute, exogenous dosing of progesterone, aldosterone, cortisol or corticosterone in Mdr1 loss-of-function mice (Mdr1 KO) resulted in higher CNS levels than WT animals (Uhr et al., 2002). Furthermore, studies on Mdr1 KO animals identified a peripheral endobiotic role and highlighted increased emotional stress in these animals (Schoenfelder et al, 2012). Thus, we investigated whether genetic or pharmacological inhibition of BBB Mdr1 may disrupt brain levels of endogenous substrates, and implicate the BBB in behavioral regulation.

To this end, we use the power of *Drosophila* genetics and complementary interrogation in mice to identify steroid partition changes in the brain and directly implicate the BBB as the cell biologic site of behavioral regulation through Mdr1 loss of function. Furthermore, acute pharmacological inhibition of Mdr1 transporters promotes CNS accumulation of selected steroids, linking genetic data to chemical biology. Finally we perform a thorough analysis of human side effects data and show that Mdr1-interacting drugs are associated with similar behavioral changes in humans. Together these findings suggest an important, evolutionarily-conserved role for BBB-localized chemoprotective ABC transporters that reaches beyond xenobiotics into endobiotic partitioning and behavioral regulation.

Results

Substrate docking and competitive transport assays suggest steroid hormones as substrates of xenobiotic efflux transporters

To determine whether *Drosophila* is a suitable model for investigating endogenous substrate partitioning roles of Mdr1-like transporters, we took an unbiased approach to compare the potential substrates of the mouse Mdr1 and the *Drosophila* homologue Mdr65. We created a homology model of Mdr65 from a mouse Mdr1 template structure and used induced fit

docking to virtually screen over 300 endogenous small molecules from the KEGG database (as in Dolghih et al, 2011). For both Mdr1 and Mdr65, docking identified endogenous substrates with potent biological functions (Fig. 1B). As previously suggested (Uhr et al., 2002, Schoenfelder et al., 2012), steroids are predicted substrates of mammalian Mdr1. Interestingly, an invertebrate steroid (ecdysone) is a highly favored substrate of the *Drosophila* Mdr65 transporter, suggesting that regulation of both xenobiotics and endogenous steroids is a conserved and important role for Mdr1-like transporters.

To determine *in vivo* whether steroids are substrates of Mdr65, we performed a competitive efflux transport assay using the active form of ecdysone, 20-hydroxyecdysone (20E), and a known fluorescent Mdr65 substrate, Rhodamine B (RhoB) (Mayer et al., 2009). We tested two conditions: RhoB in vehicle and RhoB with 20E. Mdr65 efficiently removed RhoB from wild type brains, but RhoB is retained in brains of Mdr65 mutants. Interestingly, after co-injection of RhoB and 20E, we observe a 3-fold increase in RhoB in wild type brains compared to injection of RhoB alone (Fig. 1D). Furthermore, under the same conditions, there is no significant additional increase in RhoB in Mdr65 mutant brains. These data show that 20E can compete with RhoB for its removal by Mdr65, and can function as a substrate of Mdr65.

Blood-brain barrier partitioning of 20-hydroxyecdysone is altered in Mdr65 mutant flies

We next investigated whether 20E partitioning between the hemolymph and CNS is disrupted in Mdr65 mutants. We used an ecdysone reporter fly line (EcRLBD>Stinger GFP) to visualize the presence of ecdysone in the CNS. This reporter relies on a fusion protein of the Ecdysone receptor (EcR) ligand binding domain (LBD) and the Gal4 transcription factor (Palanker et al., 2006). Upon ecdysone binding, the fusion protein translocates to the nucleus and activates transcription of nuclear-localized GFP (Stinger GFP). We first assessed the time-course of induction of GFP after hemolymph injection of 20E. GFP is efficiently induced 16 hours following 20E injection and no induction is seen after vehicle injection (Fig. 2A).

We then assessed whether 20E levels were increased in whole brain mounts from Mdr65 null mutants. In both control and Mdr65 mutant flies, hemolymph injection of 20E causes an increase in GFP fluorescence at the external surface of the brain (Fig. 2B), but GFP-positive cells are barely visible inside the brains of control flies. These data show that the reporter successfully indicates the presence of 20E in whole brain mounts, and that the wild type BBB is able to restrict 20E access into the brain. In contrast to wild type, there is an increased induction of the ecdysone reporter inside Mdr65 null mutant brains, as shown by single-plane images below the BBB (internal brain space) and at the brain cross section (Fig. 2B). The number of GFP-positive cells inside the brain is also shown for each optical section of the z-stack series (Fig. 2C). These data clearly show an increased number of GFP-positive cells, and therefore increased levels of ecdysone, inside the brains of Mdr65 mutants.

To further assess whether ecdysone levels are increased in Mdr65 mutant brains, we determined whether downstream ecdysone responses are altered. Ecdysone binds to the EcR nuclear hormone receptor, which dimerizes with the Retinoid-X receptor (RXR) homologue Ultraspiracle, and drives expression of ecdysone–responsive genes including *E74B* and

Cyp18a1 (Burtis et al., 1990, Thummel et al., 1990, Segraves and Hogness, 1990, Koelle et al., 1991, Hurban and Thummel, 1993). We find that the whole brain transcript levels of *E74B* are significantly higher in Mdr65 null brains compared to wild type brains (Fig. 2D). We also reveal metabolic consequences of diminished CNS chemoprotection as the 20E-inducible Cytochrome P450 *Cyp18a1* is increased 3-fold in Mdr65 mutant brains (Fig. 2E).

Mdr1 regulates the brain levels of Aldosterone in mice

Our findings in the *Drosophila* system and Mdr1 substrate docking predictions suggest that BBB-enriched Mdr1, the closest mouse homolog to Mdr65, might also function to inhibit blood-to-CNS flux of circulating endogenous steroids in vertebrates. As the diversity of steroids in mammals is much more sophisticated than in *Drosophila*, we took a broad and unbiased HPLC-MS/MS approach to profile the CNS levels of steroid hormones in Mdr1 mutant mice. Mice have two Mdr1 genes, Mdr1a and Mdr1b. Thus we compared the brain levels of steroids in Mdr1 double knockout mice to control mice. Our analyses show that deletion of Mdr1 does not lead to statistically significant changes in the brain levels of endogenous androstenedione, androsterone, corticosterone, dihydrotestosterone (DHT), estrone, progesterone or testosterone. However, the brains of Mdr1 mutant mice have significantly higher levels of endogenous aldosterone than brains of control mice (Aldosterone, mean of raw values: control 0.088 nM, Mdr1: 0.132 nM; relative amount (normalized to mean of control): control 100, Mdr1: 168) (Fig. 3A). This result shows that Mdr1 function is necessary for maintaining normal brain levels of aldosterone in mice.

Aldosterone is synthesized and secreted into the blood by the adrenal cortex of the adrenal gland (Bollag, 2014). Thus, the increase in brain aldosterone observed in Mdr1 mutants could be due to a steepening of the blood-to-brain gradient of aldosterone that result from an increase in blood aldosterone instead of the loss of Mdr1 efflux at the BBB. To verify that elevated aldosterone in Mdr1 mutant brains is not due to an increase in blood aldosterone, we measured steroid levels in serum as well. In contrast to brain, the serum levels of aldosterone and other steroids remain similar between Mdr1 control and mutant mice (Aldosterone, mean of raw values: control 0.573 nM, Mdr1: 0.657 nM; relative amount (normalized to mean of control): control: 100, Mdr1: 110) (Fig. 3B). These findings suggest that a steepening of the blood-to-brain gradient of aldosterone does not contribute to the observed elevation in brain aldosterone of Mdr1 mutants.

To further assess the role of Mdr1 in blood-to-brain flux of aldosterone, we tested whether acute pharmacological inhibition of Mdr1 can increase accumulation of aldosterone in the brain. For this experiment we used the established Mdr1 competitive inhibitor cyclosporin A (CsA) (Ejendal and Hrycyna, 2005, Elsinga et al., 2005) (Bakhsheshian et al., 2013, Miller, 2010). A caveat of using CsA is that it can also inhibit the BBB-enriched, efflux ABC transporter BCRP/ABCG2 (Bakhsheshian et al., 2013, Miller, 2010). Thus, we first established whether BCRP regulates the brain levels of aldosterone. As we did for Mdr1, we compared brain aldosterone levels of BCRP control and mutant mice by HPLC-MS/MS and find that aldosterone levels are similar between BCRP control and mutants (Aldosterone, mean of raw values: control: 0.088 nM, BCRP: 0.064 nM; relative amount (normalized to mean of control), control: 100, BCRP: 82) (Fig. 3C). This result shows that brain

aldosterone levels are not regulated by BCRP. Next, we tested whether acute inhibition of Mdr1 can increase the levels of aldosterone in the brain. First we intraperitoneally injected adult male wild type mice with either CsA (50 mg/Kg bw) or vehicle. One hour later, we injected all mice with aldosterone (14 mg/Kg bw) intravenously by tail vein. Three hours post aldosterone injection, we harvested brains and measured aldosterone by HPLC-MS/MS. Brains of mice treated with CsA accumulate 3.3-fold more aldosterone than brains of mice treated with vehicle (vehicle: 18.032 nM, CsA: 59.872 nM) (Fig. 3D). This result shows that acute inhibition of Mdr1 with CsA increases blood-to-brain flux of aldosterone.

Blood-brain barrier Mdr65 regulates *Drosophila* behavior

As our experiments established a conserved function for xenobiotic ABC transporters in regulating endogenous steroids in flies and mice, we investigated whether they also have conserved functions in regulating animal behavior. First, we assessed whether 20E-regulated behaviors were perturbed in flies deficient for Mdr65. It is well established that the behavioral transitions required for properly timed ecdysis and eclosion are dependent upon the precise timing of 20E peaks (Truman, 1981, Curtis et al., 1984, Truman, 1996, Zitnan et al., 1999, Zitnan et al., 2007). These behavioral transitions are also regulated, in part, by the CNS. As ecdysone is synthesized and secreted by the ring gland, which lies outside of the CNS, and is converted to active 20E by peripheral organs (Petryk et al., 2003), (Huang et al., 2008), BBB-localized Mdr65 is in a prime position to regulate CNS-related behavioral sequences required for ecdysis and eclosion. When investigating the cumulative timing of these behavioral transitions, we discover that Mdr65 mutants take 24-hours longer to reach adult eclosion (Fig. 4A).

To test whether BBB-localized Mdr65 can have cell autonomous behavioral roles, we assessed the effect of Mdr65 knock-down in the BBB. As the BBB is formed by glial cells in insects, we used pan-glial and BBB Gal4 drivers (DeSalvo et al., 2014) to express RNAi specific to Mdr65 in the BBB. Similar to the Mdr65 null mutants, but with a weaker effect, we find a statistically significant delay in adult eclosion (Fig. 4B&C). These data suggest that BBB-localized Mdr65 can regulate the behavioral transitions required for adult eclosion.

To determine whether Mdr65 can affect more complex behaviors in the adult animal, we assessed sleep behavior in Mdr65 mutants (Fig. 4D&E). 20E has a well-established dose-dependent effect on sleep/wake activity levels in *Drosophila;* increased amounts of 20E signaling in the mushroom body, a CNS substructure that controls many insect behaviors, is correlated with increased sleep intervals (Joiner et al., 2006, Pitman et al., 2006, Ishimoto and Kitamoto, 2010). We find that Mdr65 mutants demonstrate a significant increase in sleep behavior during both the daytime (27% increase) and nighttime (17% increase). Much of this increase is due to an increase in sleep bout length (Fig. 4E), a sleep characteristic that is influenced by 20E dosage (Ishimoto and Kitamoto, 2010). These data are consistent with increased 20E signaling in Mdr65 mutant brains, and suggest that BBB-localized Mdr65 can regulate complex behaviors.

Mdr1 regulates anxiety-related behaviors in mice

Next we interrogated the behavioral consequences of Mdr1 loss-of-function by comparing adult male Mdr1 mutant mice against their littermate controls in a series of tests that measure behaviors related to anxiety, motor control and social interaction.

In the novel environment exploration test Elevated Zero Maze (EZM), Mdr1 mutants spend less time in the open sections and more time in the closed sections of the EZM apparatus compared to controls (Fig. 5A). The behavior of Mdr1 mutants is consistent with an increase in anxiety levels, displaying caution when exploring a novel environment and preferring the more protected closed sections of the apparatus. Notably, the difference in behaviors between Mdr1 control and mutant mice is not due to abnormal movement or ambulation as Mdr1 controls and mutants scored similarly in these parameters (Fig. 5B).

Elevated anxiety in Mdr1 mutants was only observed when test mice (controls and mutants) were pre-exposed to the resident-intruder (RI) social interaction behavioral test (data not shown). Here, each test mouse was challenged in its home cage with a novel stimulus mouse. This gives the naïve test mice their first experience of a mouse that is not a parent or a sibling, leading to territorial, sexual and foraging competitive behaviors (Allen et al., 2010). The RI test also leads to displays of dominance and aggression, and experience of stress. These results suggest that once Mdr1 mutants experience competitiveness, dominance, aggression and/or stress from a novel male mouse, Mdr1 mutants experience above-normal anxiety in the EZM test. Similar to flies, these results show that BBB-enriched Mdr1 can modulate complex animal behaviors. Moreover, these findings suggest that Mdr1 is important for inhibiting CNS-access of molecules that can alter behavior or the development of circuitry that governs behaviors.

An association between ABC efflux transporters and anxiety-related behaviors in humans

To expand on our findings that pharmacological inhibition of mouse Mdr1 can alter BBB partitioning of aldosterone, we asked whether pharmacological modulation of this transporter can influence behavior in humans.

Activity of human Mdr1 is subject to modulation by a variety of exogenous therapeutics and endogenous binding partners. Competitive binding of Mdr1-modulating drugs may prevent Mdr1's interaction with its typical substrates, leading to adverse effects. To investigate the possible role of human Mdr1 in regulating anxiety-related behaviors, we used an established analytical approach (Liu and Altman, 2015, Lounkine et al., 2012) to calculate Mdr1's enrichment factor (EF) against each of 10,098 possible human adverse drug reactions (ADRs) gathered from the OFFSIDES collection of FDA drug reports (Tatonetti et al., 2012); Figure 6A).

In our analysis, EFs quantify how strongly a therapeutic target (e.g. Mdr1) is associated with a particular ADR. To calculate EF values, we grouped drugs known to be inhibitors (n=13) or substrates (n=36) of Mdr1, as well as OFFSIDES compounds linked to Mdr1 via ChEMBL (Supplemental Table 1), and examined whether these drugs, as a set, were enriched for certain ADRs e.g. "Anxiety" (UMLS code C00034E67) in comparison to drugs modulating other therapeutic targets. For a baseline of common drugs and their targets, we

drew from 1104 FDA approved drugs and 1884 ChEMBL targets (Gaulton et al., 2012). After filtering (see Methods), this yielded 441 FDA-approved drugs organized into 631 ChEMBL targets, with an average of 3.97 drugs ± 0.21 per target. Out of the 1,018,208 unique target-ADR pairs represented by at least one drug within the dataset, a total of only 2171 pairs (0.2%) passed our statistical threshold (EF > 1.0, q-value < 1e-4; Supplemental Table 2). Examining all targets linked to Anxiety, we find Mdr1 as one of only 12 targets significantly enriched (EF = 1.03, q-value = 1.80e-09, Fig. 6B). Furthermore, this enrichment is stable across multiple versions of ChEMBL (mean EF = 1.06 ± 0.02, Supplemental Table 3).

While we are encouraged that patient-reported anxiety findings are associated with Mdr1, albeit with a subtle effect size, we acknowledge that anxiety-like feelings could be under-represented due to subjective behavioral reporting of drug side-effects. Likewise, the ADR term “Anxiety” may not thoroughly encompass the socially-primed effects observed in the mouse. Thus, we broadened the side-effect search terms to include “Emotional Distress” (UMLS code C0700361). Strikingly, we find that Mdr1 is the 3rd most enriched target for Emotional Distress (EF = 1.28, q value = 3.39e-05, Fig. 6C) out of all 1884 targets evaluated. Thus, human behavioral regulation by this Mdr1 pathway may be broad based, consistent with previous studies noting increased emotional stress in Mdr1 mutant mice (Schoenfelder et al., 2012).

To disprove the alternative hypothesis, we used the Similarity Ensemble Approach (SEA; (Keiser et al., 2007)) and confirm that none of the 13 Mdr1 inhibitors have strongly predicted alternative off-targets more canonically associated with anxiety, such as the glucocorticoid or mineralocorticoid receptors. When expanding the analysis to include an additional 36 Mdr1 substrates, approximately 1.0% of the targets individually predicted by SEA could potentially be associated with Anxiety by literature search (Supplemental Table 5). However, none of these alternative targets achieve significant enrichment with Anxiety by EF analysis (Fig. 6B).

These results, derived from human adverse drug reaction FDA data, support our findings that modification of BBB xenobiotic efflux transporters can alter the CNS levels of CNS-active endogenous molecules and disrupt behavioral pathways.

Discussion

The Blood-brain barrier controls partitioning of biologically potent endobiotics

This study highlights the role of the BBB in regulating CNS access of circulating steroid hormones. In particular, our fly data demonstrate that disruption of Mdr65 leads to increased 20E in the CNS. In mice we also established Mdr1 as an important regulator of CNS aldosterone levels. As Mdr65 and Mdr1 have a broad spectrum of potential endogenous substrates (Fig. 1B), these findings implicate the BBB gateway in numerous small molecule regulatory events. These observations pose an intriguing hypothesis: that the BBB auto-regulates CNS chemical protection by the local sensing of altered endobiotic levels, and by triggering compensatory mechanisms to attempt to reinstate control (e.g. upregulation of Cyp18a1). This hypothesis is supported by the presence of the ecdysone receptor and

aldosterone receptor transcripts in BBB cells (Daneman et al., 2010, DeSalvo et al., 2014), which may provide a signaling mechanism to translate changes in blood composition into BBB chemoprotective response and behavioral changes. In this model, the BBB acts as a brake or buffer on the overall CNS response to normal fluctuations of peripherally synthesized hormones and other CNS-active small molecules.

ABC efflux transporters and the Blood-brain barrier are modulators of animal behaviors

Drosophila Mdr65 loss-of-function experiments reveal a significant role for ABC transporters in controlling CNS-related, ecdysone-regulated behaviors, including delayed developmental timing and increased sleep. Developmental progression is tightly regulated by precisely timed, ecdysone-induced behavioral cascades; both the rise and fall in ecdysone levels are required. The rise in 20E primes the CNS by inducing the synthesis of ecdysis-related factors; however, the secretion of these factors to trigger ecdysis only occurs after the subsequent decline in 20E titer (Truman, 1981, Curtis et al., 1984, Truman, 1996, Zitnan et al., 1999, Zitnan et al., 2007). Therefore, elevated CNS levels of 20E would be expected to cause a delay in this progression, as we see in Mdr65 mutants. Furthermore, feeding flies 20E causes an increased amount of sleep and, conversely, reducing CNS ecdysone signaling causes a reduced amount of sleep (Ishimoto and Kitamoto, 2010). Our findings are consistent with elevated CNS 20E causing increased sleep in Mdr65 mutant flies. Of note, mutation of atet, a member of the ABCG class of transporters (atet) shown to control the vesicular release of ecdysone from the main fly steroidogenic organ, led to a gross reduction in ecdysone release and availability, and a severe developmental arrest (Yamanaka et al., 2015). Our results show that even subtle changes in BBB partitioning of steroid hormones can lead to significant changes in whole animal behavior, providing the BBB with a great capacity to modulate neural functions that govern processes as complex as sleep.

Drosophila Mdr65 shares >40% sequence identity with mammalian Mdr1 and can transport Mdr1 substrates. In fact, human Mdr1 can rescue the chemoprotective BBB function of Mdr65 mutants, demonstrating that the xenobiotic-protective roles of BBB efflux transporters are conserved between flies and mammals (Mayer et al., 2009). Our data now reveals that fly Mdr65 and mouse Mdr1 also have conserved functions in regulating CNS levels of endogenous steroids as well as steroid-related CNS-governed behaviors. Moreover, we suggest that this function of ABC transporters may also manifest in human physiology.

Pharmacological modification of ABC efflux transporters provides a potential mechanism for common adverse drug reactions

We show that acute, pharmacological inhibition of Mdr1 can cause increased aldosterone in the mouse brain. We suspected that unintended therapeutic modulation of Mdr1 activity may also misregulate endogenous substrate partitioning across the BBB, leading to unexpected side effects. Consistent with this, our unbiased analysis of 1104 FDA drugs, 1884 ChEMBL targets, and 10,098 ADRs reveal links to related behavioral effects of Mdr1 inhibition: that of anxiety and emotional distress.

Admittedly, the enrichment between Mdr1 and Anxiety as a CNS side effect in humans is subtle (Fig. 6B). While in line with our observation that modification of ABC transporters

has significant CNS behavioral effects in the fly and mouse, this initial human result merits further exploration as its enrichment factor reflected several possible limitations. First, Anxiety is a widely prevalent ADR appearing for a diverse set of drugs (478 drugs: (43% of all drugs from OFFSIDES dataset). Second, few of the 1104 drugs in the dataset have been definitively characterized with respect to Mdr1, potentially confounding the analysis as unreported substrate or inhibitor roles would be expected to weaken the calculated enrichment of Mdr1 to Anxiety. Third, Mdr1 itself exhibits a broad substrate profile, as evidenced by the large number of disparate ADRs to which it is linked (216; Supplemental Table 4). Although we note that only 6% of its associated ADRs might be considered behaviorally relevant, all are taken into consideration when calculating enrichment, which can weaken Mdr1-related scores. Nevertheless, we were intrigued to see the Mdr1-Anxiety link emerge from this pan-ADR analysis at all, given these limitations. The strong enrichment between Mdr1 and Emotional Distress bypasses many of these limitations, and lends considerable support to Mdr1's potential role in stress-related behaviors.

Of note, pharmacological inhibition of Mdr1 yields no more than a 2-fold change in drug partitioning at the BBB; therefore, CNS adverse effects might seem unlikely in this context (Kalvass et al., 2013). However, our data showing that pharmacological inhibition of Mdr1 in vivo can lead to a 3.3-fold increase in brain aldosterone levels suggest that effects on endogenous molecule partitioning may be greater than previously predicted, at least transiently. Indeed, the most prevalent adverse drug reactions– altered sleep/wake cycles, depression and anxiety– run the gamut of drug classes and chemical subtypes, with no obvious common mechanism. It is possible that the same mechanisms that evolved to regulate CNS access of endogenous molecules are repurposed by the BBB to chemically isolate xenobiotics from the brain; hence, a tension occurs between endobiotic and xenobiotic partitioning during drug exposure. ABC efflux transporters are common drug targets; thus, the role of drugs in modulating the CNS entry of endogenous steroids, and their effects on behavior suggest a distinct way of thinking about complex drug-drug interactions (Zhang and Sparreboom, 2017).

In addition, genetic and environmental conditions altering human ABC transporter function may pose a previously unappreciated risk to human health. Human Mdr1 function is altered in many CNS pathologies, and single nucleotide polymorphisms (SNPs) can affect its function (Jeong et al., 2007),(Pauli-Magnus and Kroetz, 2004). For example, expression and activity levels of ABC transporters, including Mdr1, are altered in certain neurodegenerative disorders, and in normal aging (Vogelgesang et al., 2002), (Loscher and Potschka, 2005b), (Vogelgesang et al., 2006, Bauer et al., 2009, Vautier and Fernandez, 2009, Jablonski et al., 2014). Furthermore, behavioral symptoms, like anxiety and depression, are commonly associated with these disorders (Chemerinski et al., 1998). Thus, altered endobiotic pharmacokinetics at the BBB may provide a mechanism for these clinical manifestations. Further study of BBB regulated processes may yield other roles for BBB function in behavior, and new systems for targeting behavioral therapies that are more accessible than internal brain pathways.

Experimental Procedures

Homology Modeling

The protein sequence of Mdr65 was obtained from the Uniprot database, accession number Q000748. The structure of mouse Mdr1 with docked saquinavir sharing 40% sequence identity with Mdr65, was used as the template (PDB ID 3G60). Sequence alignment was performed using BLAST, and the Mdr65 model was built using the standard homology protocol within the Prime module of Schrodinger Suite 2012. The model was subsequently processed in the Prepwizard module to optimize hydrogens; the model was subsequently subjected to restrained energy minimization with the saquinavir ligand removed.

Ligand Docking

Flexible receptor docking was performed using the induced fit docking protocol developed previously (Dolghih et al., 2011) and final scoring was implemented using the extra precision (XP) Glide with the OPLS2005 force field. A 10 × 10 × 10 Å inner docking box with the center at coordinates (19.0, 46.0, −6.0) Å was used. The number of poses saved during the initial docking was set to 100. In the next stage, only residues within 5 Å of each ligand were minimized and up to 20 top poses were saved and scored with Glide XP.

Ligands

Ligand structures were obtained from the KEGG database of biologically relevant molecules and processed using the *Ligprep* 2.4 module. Parameters were assigned based on the OPLS2005 force field. Ionization states were assigned by *Epik*, and groups with pKa between 5 and 9 were treated as neutral while those outside the range were treated as charged.

Drosophila genetics

The following fly strains were used during this study: Canton-S and isogenized w^{-1118} (w-ISO) wild type strains, the EcRLBD ecdysone reporter stock #23656, UAS-StingerGFP (generated from stock #28863), and repo-Gal4 stock #7415 (Bloomington Drosophila Stock Center), the pMdr65 null mutant strain KG08723 (Drosophila Genetic Resource Center), the UAS-Mdr65RNAi Stock #9019 (Vienna Drosophila Research Center (Dietzl et al., 2007)), and 9-137 Gal4 (DeSalvo et al., 2014).

In vivo competitive efflux transport assay

4-8d old male flies were hemolymph-injected (Mayer et al., 2009) with 200 ng Rhodamine B (R6626; Sigma) and either 20% ethanol (vehicle) or approximately 500 ng (~100 nl of 4.8 mg/ml) 20-hydroxyecdysone (20E; H5142; Sigma). Flies were left for 2 h followed by rapid dissection of the brains in PBS (<2 min per dissection). The brains were rinsed in PBS, immediately placed in individual wells of a foil-covered fluorometer plate containing 200 µ 10% SDS, then left to dissociate for 30 min followed by fluorimetry (ex. 535 nm/em. 595 nm). Brain fluorescence readings were normalized to whole body readings to account for individual differences in dye loading and elimination from the fly. N=7 (except for n=4 for the Mdr65 RhoB/20E condition).

Western blotting

For the EcRLBD reporter time-course assays, 4-8d old male flies were hemolymph-injected with 20% ethanol (vehicle) or 4.8 mg/ml 20E and were frozen after specified time-points. Heads were isolated and homogenized in sample buffer (0.04% Bromophenol Blue, 4% SDS, 4% glycerol, 10% β-mercaptoethanol, 0.1M Tris, pH 6.8). The equivalent of two fly heads was run for each time-point. Western analysis was performed using standard 10% PAGE gels blotted onto PVDF membranes (BioRad) and blocked using 5% non-fat milk in Tris-buffered saline supplemented with 0.1% Tween-20 (0.1% TBS-T) for 1 h. Primary antibody hybridization occurred overnight at 4°C followed by 3× washes in 0.1% TBS-T, secondary antibody hybridization for 1 h, then 3× washes in 0.1% TBS-T. Primary antibodies: rabbit α-GFP (1:1000; ab6556; Abcam) and mouse α-tubulin (1:100; E7; DSHB). Secondary antibodies: goat α-rabbit HRP (1:40,000; #28177; AnaSpec) and goat α-mouse HRP (1:1000; #31430; Pierce).

Immunofluorescence

4-8d old male flies were hemolymph-injected with 12.5 μg/μl 70 kDa Texas Red dextran (D1864; Invitrogen) and either 20% ethanol (vehicle) or approximately 500 ng 20E with overnight recovery (approximately 16 h). Heads were bisected from the bodies, the proboscis discarded, and then fixed in 3.7% paraformaldehyde/PBS for 15 min. Brains were dissected in PBS, removing the fat bodies and large trachea, washed in PBS followed by incubation in blocking buffer (5% normal calf serum or donkey serum, 4% Tween-20 in PBS) for 1 h, then primary antibody incubation overnight at 4°C. Brains were washed in PBS (3× 30 min), incubated in secondary antibody for 45 min, washed in PBS (3× 45 min) and mounted in Dako fluorescent mounting medium (S3023; Dako) on glass slides with nail polish posts. Brains were imaged immediately using a Zeiss LSM 510 confocal microscope. Primary antibodies: rabbit α-GFP polyclonal (1:1000; ab6556; Abcam), mouse α-repo monoclonal (1:10; 8D12; Developmental Studies Hybridoma Bank (DSHB)). Secondary antibodies: goat α-rabbit FITC (1:100; Invitrogen), goat α-mouse Cy5 (1:1000; ab6563; Abcam), donkey α-rabbit Alexa Fluor 488 (1:1000; Invitrogen), donkey α-mouse Alexa Fluor 647 (1:1000; Invitrogen). Confocal z-section images were acquired every 0.5 μm from the BBB surface through to the cross-section. Confocal settings were maintained across all samples within an experiment. At least 3 brains were imaged per condition, and data analyzed from at least 3 technical replicates.

Image analyses

Quantification of GFP-positive cells in the CNS of Mdr65 mutants and controls were calculated using ImageJ. Z-stack section TIFF files were converted to binary (8-bit) and identical threshold settings were applied. Data were normalized to the number of GFP-positive cells at the brain surface.

Developmental timing and eclosion

Vials containing 20 males and females were transferred to fresh food with added yeast paste every 2 h at 25°C to allow egg laying. Flies were maintained at 25°C except when scoring once per day. At least 2 technical replicates were performed. For the BBB knock-down of

Mdr65, the eclosion assays were performed in bottles and the flies were left to lay eggs for approximately 2 days. The number of hatched flies was scored twice daily and the numbers pooled per day. At least 2 technical replicates were performed.

Sleep analysis

Newly eclosed flies were collected under brief CO_2 anesthesia over a 3-day period. Males were housed with 10 flies per vial on standard cornmeal agar media, and aged for 3-5 days. For sleep analysis, flies were individually aspirated into a glass tube (5 [W] × 65 [L] mm) with regular fly food, and their locomotor activity was monitored using the Drosophila Activity Monitoring (DAM) system (Trikinetics, Waltham, MA, USA) while subjected to 12 hr light and 12 hr dark cycles at 25°C with 65% humidity. Flies were acclimated to the experimental conditions for one day before sleep was analyzed. Locomotor activity data were collected at 1-min intervals for 3 days, and analyzed with a Microsoft (Redmond, WA, USA) Excel-based macro program as described previously (Hendricks et al., 2003), (Kume et al., 2005). A sleep bout was defined as 5 or more minutes of behavioral immobility. N=64 flies/genotype.

QPCR

Total RNA was extracted from male brains (4 brains/replicate) using the RNAqueous Micro kit (AM1931; Ambion). Manufacturer's instructions were followed except the lysates were reloaded after the initial filtration, to increase RNA binding, and the RNA was eluted using 75°C RNas e-free water (AM9938; Ambion). Following DNase treatment, equal amounts of RNA were reverse-transcribed to cDNA (30-40 ng) using the Superscript III First Strand kit (18080-051; Invitrogen) according to manufacturer's instructions. QPCR was performed using a 1/10 dilution of the cDNA. The following oligos were used to assess *E74B* and *Cyp18a1* levels in *Drosophila* brains:

mRPS24 Fw: GAACACGTCAACAATGAAGGA

mRPS24 Rv: ACAAACTTGCGGATGAACAC

Aps Fw: GTGTATTCGAGAACAATGACCA

Aps Rv: GTCACGTTCATCACGAACAC

Glo Fw: AATTGGGCACAGGTATATTGAG

Glo Rv: CTCTTCATTTCAGCAATCGAG

E74B Fw: ATCGGCGGCCTACAAGAAG (Caldwell et al., 2005),(Neuman et al., 2014)

E74B Rv: TCGATTGCTTGACAATAGGAATTTC (Caldwell et al., 2005),(Neuman et al., 2014)

Cyp18a1 Fw: 933 AAGAATCACGAGGAGCAACTG

Cyp18a1 Rv: 1033 AGCATGAACACGTTTATCCAC

For each cDNA sample, the data were normalized to the geometric mean of three reference genes (mRPS24, Aps and Glo) as described in Vandesompele *et al.* (2002). The following

annealing temperatures were used: 60°C (mRpS24), 59°C (E74B), 56°C (Cyp18a1) and 53°C (Glo and Aps). Statistical analyses were performed using an unpaired t-test in GraphPad Prism 6 software. At least 3 biological replicates and 3 technical replicates were performed.

Statistical analyses for *Drosophila* studies

Statistical analysis of the *Drosophila* fluorometry data was performed using a Dixon's Q-test, which identified one outlier for removal (Q_{exp} = 0.726, with Q_{crit} = 0.680 at CL:99% for N=7), followed by a one-way ANOVA using a Sidak post-hoc test in Graphpad Prism software. Microsoft Excel was used for statistical analyses of QPCR and all behavioral assays using unpaired, two-tailed T tests.

Mice

Mouse lines FVB, 1487 (Mdr1a−/−; Mdr1b−/− (Mdr1)) and 2767 (BCRP$^{-/-}$) were purchased from Taconic. Mice bred to maintain homozygosity or purchased were used for non-behavioral experiments. For behavioral experiments, matings starting with FVB and Mdr1 mice were used to generate Mdr1 controls (Mdr1a+/+;Mdr1b+/+ and Mdr1a+/−; Mdr1b+/−) and Mdr1 mutants (Mdr1a−/−; Mdr1b−/−). C57BL/6 mice used as "intruder" were purchased from Simonsen. All mouse protocols were approved by the UCSF and UCSD Institutional Animal Care and Use Committee.

Collection of mouse brain and blood

Samples were collected from 3.5-month-old males. Mice were anesthetized with ketamine/xylazine/acepromazine maleate mix at 100/6/1mg per Kg mass prior to surgery. Procedures for collecting blood that reduce red blood cell lysis were used. Excess peritoneal fluid was removed through a small opening in the abdomen to prevent flow of fluid into chest cavity, the chest cavity opened, the right atrium cut, and blood pooled in the chest cavity was pipetted with an enlarged-bore tip. Animals were then perfused with cold DPBS to remove blood. Whole brains were dissected, immediately placed in a microcentrifuge tube, frozen in dry ice, and homogenized for analysis or placed at −80°C for later homogenization. Control and mutant samples were collected concurrently.

Serum preparation for mouse samples

Freshly collected blood was incubated at 37°C for 1 5 min then at 4°C for 1h to promote clotting. Clotted blood was centrifuged at 4°C, 5000 RCF for 10 min. Straw-colored supernatant was collected and centrifuged at 4°C, 7500 RCF for 10 min. Supernatant was then collected and stored at −80°C.

Mass Spectrometry for mouse samples

Targeted metabolites were measured by HPLC tandem mass spectrometry (HPLC-MS/MS) in multiple reaction monitoring mode (MRM) using a SCIEX API 4000 QTrap by Biocrates Life Sciences AG. Seven-point external calibration curves and 13 isotope-labeled internal standards were used. Metabolite concentrations of each sample were determined in a single

analysis. Serum samples were directly used for analyses. Brain tissue samples were extracted for steroids using a fixed ratio of extraction volume to weight.

Pharmacological inhibition of Mdr1

Adult male FVB mice were injected with cyclosporin A (Cell Signaling 9973S; solubilized in 100% DMSO at 50mg/Kg body weight (bw)) or vehicle intraperitoneally at time zero (T=0). All mice were then injected with aldosterone (Sigma A9477; solubilized in 6.25% ethanol and 6.25% DMSO at 14mg/Kg bw) intravenously by tail vein at T=1hr. The amounts of ethanol and DMSO given to mice were below the LD50 for both chemicals. The following conditions were compared: 1) vehicle followed by aldosterone, 2) cyclosporin A followed by aldosterone. At T=4hr, brains were collected and analyzed by HPLC-MS/MS as described above.

Behavioral tests for mice

Control and mutant male mice used for behavioral tests were born and raised in our animal facility, weaned at age P20, housed with male siblings until social isolation (SI) 3-7 days prior to first behavioral test at 3.5 months of age. Animals were raised with 12:12 hour light:dark cycle. Two sets of behavioral tests were conducted: 1) Open Field (OF)-Elevated Zero Maze (EZM): SI 3 days prior to OF, 2 days SI until EZM. A single cohort of control and mutant mice were tested together. 2) Resident Intruder (RI)-OF-EZM: SI for 7 days prior to RI, 4-5 days SI until OF, 2 days SI until EZM. Two cohorts were tested on different days. Mice were acclimated in the testing room 25-45 minutes before tests. EZM tests were conducted at the UCSF Neurobehavioral Core for Rehabilitation Research during 9am–1pm of the light cycle. Apparatus: 5cm wide circular track of 21.25cm outer diameter, 80cm high with 42cm long open or closed sections, 31 surface infrared beams. Genotypes were blind to operators. Kinder Scientific infrared-detection apparatus and Motor Monitor software were used for behavioral tests. Tests were performed with the operator either in a different room or out of sight from mice being tested, in an activity-absent room with ~70 decibels of white noise.

Statistical analyses for mouse studies

Graphpad Prism software was used for statistical analyses of mass spectrometry and animal behavior data using unpaired, nonparametric Mann-Whitney tests.

Associations between targets and ADRs

We collected 10,098 documented ADRs for 1,332 FDA-approved drugs from the OFFSIDES database (Tatonetti et al., 2012). To avoid duplicates, we standardized and converted each drug to its InChIKey, yielding 1104 unique drug structures. ADRs were considered associated with a drug if OFFSIDES reported a p-value for the drug-ADR link of $p < 1\times10^{-2}$; this yielded 9366 unique drug-ADR pairs. We then identified all known human targets for all drugs using ChEMBL (Version 17; (Gaulton et al., 2012)). Targets were considered “known” if a documented ligand for the target had a Tanimoto Coefficient of 1.0 with the drug in question; this yielded 805 (out of 1884 possible) unique targets, 631 of which were human. An initial filter required all drugs to have an association with both an

ADR and a target to be considered for analysis (441 drugs, post-filter). In total there were 6,780,515 unique drug-target-ADR triplets. Each unique target-ADR pair had to occur at least 10 times before being considered for enrichment. All resulting drug-ADR (315,279), drug-target (3136), and target-ADR (1,018,208) pairs were then enumerated. An enrichment factor (EF) was calculated for each target-ADR pair after correction for multiple hypothesis testing using the Benjamini-Hochberg method as previously described (Lounkine et al., 2012).

Alternate target predictions

We used the Similarity Ensemble Approach (Keiser et al., 2007) with RDKit (rdkit.org) ECFP4 (Morgan) and path-based fingerprints to identify predicted additional off-targets of all Mdr1 inhibitors (Supplemental Table 5) and substrates.

Supplementary Material

Refer to Web version on PubMed Central for supplementary material.

Acknowledgments

R.N.M. was funded by UCSF Dept. of Clinical Pharmacology and Therapeutics (GM007546) and Dept. of Anesthesia and Perioperative Care (GM008440) NIH T32 grants. R.J.B. was supported by NIH GRANTs R01GM081863 and R21NS082856, NIEHS R21 ES021412, the UCSF Department of Anesthesia and Perioperative Care, and the Sandler foundation. R.D. was funded by the UCSF Program for Breakthrough Biomedical Research. M.J.K. was funded by a NIH SBIR (GM093456) and a Glenn Foundation Award for Research in Biological Mechanisms of Aging. G.G. was supported by iPQB Bioinformatics Training Grant. T.K. was funded by a NSF grant (IOS1352882). M.P.J. was funded by a NIH P01 grant (GM111126). M.P.J. is a consultant to Schrodinger LLC, which licenses, develops, and distributes software used in this work. We would like to acknowledge members of the Kenyon and O'Farrell labs for critical reading of the manuscript and helpful suggestions. We would also like to thank members of the Bainton, Daneman and Kroetz labs for technical assistance and useful guidance during this work.

Abbreviations

20-E	20-hydroxyecdysone
ABC	ATP-binding Cassette
ADRs	Adverse Drug Reactions
BBB	Blood-Brain Barrier
BVEC	brain vascular endothelial cells
CNS	central nervous system
EcRLBD	ecdysone receptor ligand binding domain
EF	enrichment factor
MDR	multidrug resistant
RhoB	Rhodamine B
SPG	Subperineurial glia

References

ALLEN AEC, CRAGG CL, WOOD AJ, PFAFF DW, CHOLERIS E. Agonistic behavior in males and females: Effects of an estrogen receptor beta agonist in gonadectomized and gonadally intact mice. Psychoneuroendocrinology. 2010; 35:1008–1022. [PubMed: 20129736]

BAKHSHESHIAN J, HALL MD, ROBEY RW, HERRMANN MA, CHEN JQ, BATES SE, GOTTESMAN MM. Overlapping substrate and inhibitor specificity of human and murine ABCG2. Drug Metab Dispos. 2013; 41:1805–12. [PubMed: 23868912]

BAUER M, KARCH R, NEUMANN F, ABRAHIM A, WAGNER CC, KLETTER K, MULLER M, ZEITLINGER M, LANGER O. Age dependency of cerebral P-gp function measured with (R)-[11C]verapamil and PET. Eur J Clin Pharmacol. 2009; 65:941–6. [PubMed: 19655132]

BOLLAG WB. Regulation of aldosterone synthesis and secretion. Compr Physiol. 2014; 4:1017–55. [PubMed: 24944029]

BURTIS KC, THUMMEL CS, JONES CW, KARIM FD, HOGNESS DS. The Dm 74EF early puff contains E74, a complex ecdysone-inducible gene that encodes two ets-related proteins. Cell. 1990; 61:85–99. [PubMed: 2107982]

CALDWELL PE, WALKIEWICZ M, STERN M. Ras activity in the Dm prothoracic gland regulates body size and developmental rate via ecdysone release. Curr Biol. 2005; 15:1785–95. [PubMed: 16182526]

CHEMERINSKI E, PETRACCA G, MANES F, LEIGUARDA R, STARKSTEIN SE. Prevalence and correlates of anxiety in Alzheimer's disease. Depress Anxiety. 1998; 7:166–70. [PubMed: 9706453]

CORDON-CARDO C, O'BRIEN JP, CASALS D, RITTMAN-GRAUER L, BIEDLER JL, MELAMED MR, BERTINO JR. Multidrug-resistance gene (P-glycoprotein) is expressed by endothelial cells at blood-brain barrier sites. Proc Natl Acad Sci U S A. 1989; 86:695–8. [PubMed: 2563168]

CURTIS, AT., HORI, M., GREEN, JM., WOLFGANG, WJ., HIRUMA, K., RIDDIFORD, LM. Journal of Insect Physiology. Vol. 30. &: 1984. Ecdysteroid Regulation of the Onset of Cuticular Melanization in Allatectomized and Black Mutant Manduca-Sexta Larvae; p. 597

DANEMAN R. The blood-brain barrier in health and disease. Ann Neurol. 2012; 72:648–72. [PubMed: 23280789]

DANEMAN R, ZHOU L, AGALLIU D, CAHOY JD, KAUSHAL A, BARRES BA. The mouse blood-brain barrier transcriptome: a new resource for understanding the development and function of brain endothelial cells. PLoS One. 2010; 5:e13741. [PubMed: 21060791]

DESALVO MK, HINDLE SJ, RUSAN ZM, ORNG S, EDDISON M, HALLIWELL K, BAINTON RJ. The Dm surface glia transcriptome: evolutionary conserved blood-brain barrier processes. Frontiers in Neuroscience. 2014; 8

DIETZL G, CHEN D, SCHNORRER F, SU KC, BARINOVA Y, FELLNER M, GASSER B, KINSEY K, OPPEL S, SCHEIBLAUER S, COUTO A, MARRA V, KELEMAN K, DICKSON BJ. A genome-wide transgenic RNAi library for conditional gene inactivation in Dm. Nature. 2007; 448:151–6. [PubMed: 17625558]

DOLGHIH E, BRYANT C, RENSLO AR, JACOBSON MP. Predicting binding to p-glycoprotein by flexible receptor docking. PLoS Comput Biol. 2011; 7:e1002083. [PubMed: 21731480]

EJENDAL KF, HRYCYNA CA. Differential sensitivities of the human ATP-binding cassette transporters ABCG2 and P-glycoprotein to cyclosporin A. Mol Pharmacol. 2005; 67:902–11. [PubMed: 15598974]

ELSINGA PH, HENDRIKSE NH, BART J, VAN WAARDE A, VAALBURG W. Positron emission tomography studies on binding of central nervous system drugs and P-glycoprotein function in the rodent brain. Mol Imaging Biol. 2005; 7:37–44. [PubMed: 15912274]

FORD JM. Experimental reversal of P-glycoprotein-mediated multidrug resistance by pharmacological chemosensitisers. Eur J Cancer. 1996; 32A:991–1001. [PubMed: 8763340]

GAULTON A, BELLIS LJ, BENTO AP, CHAMBERS J, DAVIES M, HERSEY A, LIGHT Y, MCGLINCHEY S, MICHALOVICH D, AL-LAZIKANI B, OVERINGTON JP. ChEMBL: a large-scale bioactivity database for drug discovery. Nucleic Acids Res. 2012; 40:D1100–7. [PubMed: 21948594]

HENDRICKS JC, LU S, KUME K, YIN JC, YANG Z, SEHGAL A. Gender dimorphism in the role of cycle (BMAL1) in rest, rest regulation, and longevity in Dm melanogaster. J Biol Rhythms. 2003; 18:12–25. [PubMed: 12568241]

HINDLE SJ, BAINTON RJ. Barrier mechanisms in the Dm blood-brain barrier. Front Neurosci. 2014; 8:414. [PubMed: 25565944]

HUANG X, WARREN JT, GILBERT LI. New players in the regulation of ecdysone biosynthesis. J Genet Genomics. 2008; 35:1–10. [PubMed: 18222403]

HURBAN P, THUMMEL CS. Isolation and characterization of fifteen ecdysone-inducible Dm genes reveal unexpected complexities in ecdysone regulation. Mol Cell Biol. 1993; 13:7101–11. [PubMed: 8413299]

ISHIMOTO H, KITAMOTO T. The steroid molting hormone Ecdysone regulates sleep in adult Dm melanogaster. Genetics. 2010; 185:269–81. [PubMed: 20215472]

JABLONSKI M, MILLER DS, PASINELLI P, TROTTI D. ABC transporter-driven pharmacoresistance in Amyotrophic Lateral Sclerosis. Brain Res. 2014

JEONG H, HERSKOWITZ I, KROETZ DL, RINE J. Function-altering SNPs in the human multidrug transporter gene ABCB1 identified using a Saccharomyces-based assay. PLoS Genet. 2007; 3:e39. [PubMed: 17352537]

JOINER WJ, CROCKER A, WHITE BH, SEHGAL A. Sleep in Dm is regulated by adult mushroom bodies. Nature. 2006; 441:757–60. [PubMed: 16760980]

KALVASS JC, POLLI JW, BOURDET DL, FENG B, HUANG SM, LIU X, SMITH QR, ZHANG LK, ZAMEK-GLISZCZYNSKI MJ, INTERNATIONAL TRANSPORTER, C. Why clinical modulation of efflux transport at the human blood-brain barrier is unlikely: the ITC evidence-based position. Clin Pharmacol Ther. 2013; 94:80–94. [PubMed: 23588303]

KEISER MJ, ROTH BL, ARMBRUSTER BN, ERNSBERGER P, IRWIN JJ, SHOICHET BK. Relating protein pharmacology by ligand chemistry. Nat Biotechnol. 2007; 25:197–206. [PubMed: 17287757]

KOELLE MR, TALBOT WS, SEGRAVES WA, BENDER MT, CHERBAS P, HOGNESS DS. The Dm EcR gene encodes an ecdysone receptor, a new member of the steroid receptor superfamily. Cell. 1991; 67:59–77. [PubMed: 1913820]

KUME K, KUME S, PARK SK, HIRSH J, JACKSON FR. Dopamine is a regulator of arousal in the fruit fly. J Neurosci. 2005; 25:7377–84. [PubMed: 16093388]

LIU T, ALTMAN RB. Relating Essential Proteins to Drug Side-Effects Using Canonical Component Analysis: A Structure-Based Approach. J Chem Inf Model. 2015; 55:1483–94. [PubMed: 26121262]

LOSCHER W, POTSCHKA H. Blood-brain barrier active efflux transporters: ATP-binding cassette gene family. NeuroRx. 2005a; 2:86–98. [PubMed: 15717060]

LOSCHER W, POTSCHKA H. Drug resistance in brain diseases and the role of drug efflux transporters. Nat Rev Neurosci. 2005b; 6:591–602. [PubMed: 16025095]

LOUNKINE E, KEISER MJ, WHITEBREAD S, MIKHAILOV D, HAMON J, JENKINS JL, LAVAN P, WEBER E, DOAK AK, COTE S, SHOICHET BK, URBAN L. Large-scale prediction and testing of drug activity on side-effect targets. Nature. 2012; 486:361–7. [PubMed: 22722194]

MAYER F, MAYER N, CHINN L, PINSONNEAULT RL, KROETZ D, BAINTON RJ. Evolutionary conservation of vertebrate blood-brain barrier chemoprotective mechanisms in Dm. J Neurosci. 2009; 29:3538–50. [PubMed: 19295159]

MILLER DS. Regulation of P-glycoprotein and other ABC drug transporters at the blood-brain barrier. Trends Pharmacol Sci. 2010; 31:246–54. [PubMed: 20417575]

MULLER MB, KECK ME, BINDER EB, KRESSE AE, HAGEMEYER TP, LANDGRAF R, HOLSBOER F, UHR M. ABCB1 (MDR1)-type P-glycoproteins at the blood-brain barrier modulate the activity of the hypothalamic-pituitary-adrenocortical system: implications for affective disorder. Neuropsychopharmacology. 2003; 28:1991–9. [PubMed: 12888779]

NAITO M, YUSA K, TSURUO T. Steroid hormones inhibit binding of Vinca alkaloid to multidrug resistance related P-glycoprotein. Biochem Biophys Res Commun. 1989; 158:1066–71. [PubMed: 2563940]

NEUMAN SD, IHRY RJ, GRUETZMACHER KM, BASHIRULLAH A. INO80-dependent regression of ecdysone-induced transcriptional responses regulates developmental timing in Dm. Dev Biol. 2014; 387:229–39. [PubMed: 24468295]

PALANKER L, NECAKOV AS, SAMPSON HM, NI R, HU C, THUMMEL CS, KRAUSE HM. Dynamic regulation of Dm nuclear receptor activity in vivo. Development. 2006; 133:3549–62. [PubMed: 16914501]

PAULI-MAGNUS C, KROETZ DL. Functional implications of genetic polymorphisms in the multidrug resistance gene MDR1 (ABCB1). Pharm Res. 2004; 21:904–13. [PubMed: 15212152]

PETRYK A, WARREN JT, MARQUES G, JARCHO MP, GILBERT LI, KAHLER J, PARVY JP, LI Y, DAUPHIN-VILLEMANT C, O'CONNOR MB. Shade is the Dm P450 enzyme that mediates the hydroxylation of ecdysone to the steroid insect molting hormone 20-hydroxyecdysone. Proc Natl Acad Sci U S A. 2003; 100:13773–8. [PubMed: 14610274]

PITMAN JL, MCGILL JJ, KEEGAN KP, ALLADA R. A dynamic role for the mushroom bodies in promoting sleep in Dm. Nature. 2006; 441:753–6. [PubMed: 16760979]

SCHOENFELDER Y, HIEMKE C, SCHMITT U. Behavioural consequences of p-glycoprotein deficiency in mice, with special focus on stress-related mechanisms. J Neuroendocrinol. 2012; 24:809–17. [PubMed: 22339976]

SEGRAVES WA, HOGNESS DS. The E75 ecdysone-inducible gene responsible for the 75B early puff in Dm encodes two new members of the steroid receptor superfamily. Genes Dev. 1990; 4:204–19. [PubMed: 2110921]

SILBERMANN MH, BOERSMA AW, JANSSEN AL, SCHEPER RJ, HERWEIJER H, NOOTER K. Effects of cyclosporin A and verapamil on the intracellular daunorubicin accumulation in Chinese hamster ovary cells with increasing levels of drug-resistance. Int J Cancer. 1989; 44:722–6. [PubMed: 2477337]

STORK T, ENGELEN D, KRUDEWIG A, SILIES M, BAINTON RJ, KLAMBT C. Organization and function of the blood-brain barrier in Dm. J Neurosci. 2008; 28:587–97. [PubMed: 18199760]

TATONETTI NP, YE PP, DANESHJOU R, ALTMAN RB. Data-driven prediction of drug effects and interactions. Sci Transl Med. 2012; 4:125ra31.

THIEBAUT F, TSURUO T, HAMADA H, GOTTESMAN MM, PASTAN I, WILLINGHAM MC. Cellular localization of the multidrug-resistance gene product P-glycoprotein in normal human tissues. Proc Natl Acad Sci U S A. 1987; 84:7735–8. [PubMed: 2444983]

THUMMEL CS, BURTIS KC, HOGNESS DS. Spatial and temporal patterns of E74 transcription during Dm development. Cell. 1990; 61:101–11. [PubMed: 1690603]

TRUMAN JW. Interaction between Ecdysteroid, Eclosion Hormone, and Bursicon Titers in Manduca-Sexta. American Zoologist. 1981; 21:655–661.

TRUMAN JW. Ecdysis control sheds another layer. Science. 1996; 271:40–41. [PubMed: 8539597]

TSUKITA S, FURUSE M, ITOH M. Multifunctional strands in tight junctions. Nat Rev Mol Cell Biol. 2001; 2:285–93. [PubMed: 11283726]

TSURUO T II, DA H, NOJIRI M, TSUKAGOSHI S, SAKURAI Y. Circumvention of vincristine and Adriamycin resistance in vitro and in vivo by calcium influx blockers. Cancer Res. 1983; 43:2905–10. [PubMed: 6850602]

TSURUO T II, DA H, TSUKAGOSHI S, SAKURAI Y. Increased accumulation of vincristine and adriamycin in drug-resistant P388 tumor cells following incubation with calcium antagonists and calmodulin inhibitors. Cancer Res. 1982a; 42:4730–3. [PubMed: 7127307]

TSURUO T II, DA H, YAMASHIRO M, TSUKAGOSHI S, SAKURAI Y. Enhancement of vincristine- and adriamycin-induced cytotoxicity by verapamil in P388 leukemia and its sublines resistant to vincristine and adriamycin. Biochem Pharmacol. 1982b; 31:3138–40. [PubMed: 7150340]

UEDA K, OKAMURA N, HIRAI M, TANIGAWARA Y, SAEKI T, KIOKA N, KOMANO T, HORI R. Human P-glycoprotein transports cortisol, aldosterone, and dexamethasone, but not progesterone. J Biol Chem. 1992; 267:24248–52. [PubMed: 1360010]

UHR M, HOLSBOER F, MULLER MB. Penetration of endogenous steroid hormones corticosterone, cortisol, aldosterone and progesterone into the brain is enhanced in mice deficient for both mdr1a

and mdr1b P-glycoproteins. Journal of Neuroendocrinology. 2002; 14:753–759. [PubMed: 12213137]

VAN ASPEREN J, SCHINKEL AH, BEIJNEN JH, NOOIJEN WJ, BORST P, VAN TELLINGEN O. Altered pharmacokinetics of vinblastine in Mdr1a P-glycoprotein-deficient Mice. J Natl Cancer Inst. 1996; 88:994–9. [PubMed: 8667431]

VANDESOMPELE J, DE PRETER K, PATTYN F, POPPE B, VAN ROY N, DE PAEPE A, SPELEMAN F. Accurate normalization of real-time quantitative RT-PCR data by geometric averaging of multiple internal control genes. Genome Biol. 2002; 3 RESEARCH0034.

VAUTIER S, FERNANDEZ C. ABCB1: the role in Parkinson's disease and pharmacokinetics of antiparkinsonian drugs. Expert Opin Drug Metab Toxicol. 2009; 5:1349–58. [PubMed: 19663741]

VOGELGESANG S, CASCORBI I, SCHROEDER E, PAHNKE J, KROEMER HK, SIEGMUND W, KUNERT-KEIL C, WALKER LC, WARZOK RW. Deposition of Alzheimer's beta-amyloid is inversely correlated with P-glycoprotein expression in the brains of elderly non-demented humans. Pharmacogenetics. 2002; 12:535–41. [PubMed: 12360104]

VOGELGESANG S, GLATZEL M, WALKER LC, KROEMER HK, AGUZZI A, WARZOK RW. Cerebrovascular P-glycoprotein expression is decreased in Creutzfeldt-Jakob disease. Acta Neuropathol. 2006; 111:436–43. [PubMed: 16523342]

YAMANAKA N, MARQUES G, O'CONNOR MB. Vesicle-Mediated Steroid Hormone Secretion in Drosophila melanogaster. Cell. 2015; 163:907–19. [PubMed: 26544939]

ZHANG L, SPARREBOOM A. Predicting transporter-mediated drug interactions: Commentary on: "Pharmacokinetic evaluation of a drug transporter cocktail consisting of digoxin, furosemide, metformin and rosuvastatin" and "Validation of a microdose probe drug cocktail for clinical drug interaction assessments for drug transporters and CYP3A". Clin Pharmacol Ther. 2017; 101:447–449. [PubMed: 27981558]

ZITNAN D, KIM YJ, ZITNANOVA I, ROLLER L, ADAMS ME. Complex steroid-peptide-receptor cascade controls insect ecdysis. Gen Comp Endocrinol. 2007; 153:88–96. [PubMed: 17507015]

ZITNAN D, ROSS LS, ZITNANOVA I, HERMESMAN JL, GILL SS, ADAMS ME. Steroid induction of a peptide hormone gene leads to orchestration of a defined behavioral sequence. Neuron. 1999; 23:523–35. [PubMed: 10433264]

Highlights

- Blood-brain barrier ABC drug transporters regulate CNS levels of steroids
- Blood-brain barrier ABC drug transporters regulate whole animal behavior
- Stress-related drug side-effects are associated with the ABC drug transporter Mdr1
- Competitive Mdr1 drug/steroid interactions may shed light on adverse drug reactions

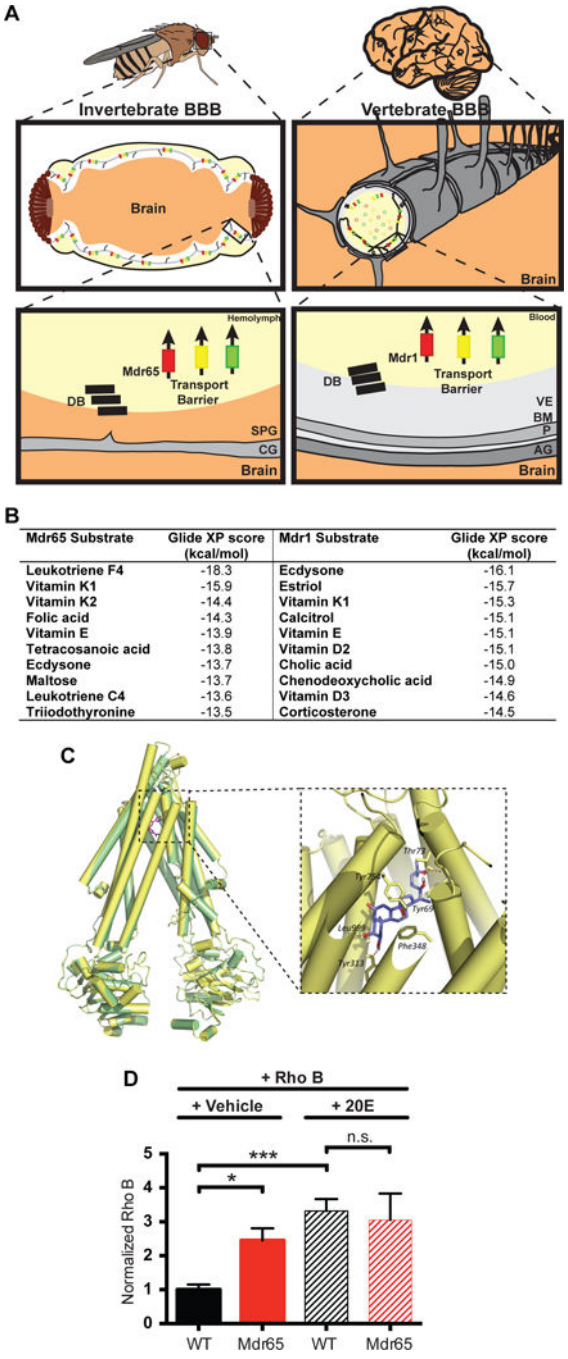

Mdr65 Substrate	Glide XP score (kcal/mol)	Mdr1 Substrate	Glide XP score (kcal/mol)
Leukotriene F4	-18.3	Ecdysone	-16.1
Vitamin K1	-15.9	Estriol	-15.7
Vitamin K2	-14.4	Vitamin K1	-15.3
Folic acid	-14.3	Calcitrol	-15.1
Vitamin E	-13.9	Vitamin E	-15.1
Tetracosanoic acid	-13.8	Vitamin D2	-15.1
Ecdysone	-13.7	Cholic acid	-15.0
Maltose	-13.7	Chenodeoxycholic acid	-14.9
Leukotriene C4	-13.6	Vitamin D3	-14.6
Triiodothyronine	-13.5	Corticosterone	-14.5

Figure 1. The *Drosophila* steroid 20-hydroxyecdysone is a predicted Mdr65 substrate

(A) Diagram of the invertebrate and vertebrate blood-brain barrier. The invertebrate BBB is a compound structure, formed by subperineurial glia (SPG), outer perineurial glia, and a basement membrane; only the SPG are shown for simplicity. The vertebrate BBB is primarily formed by the brain vascular endothelial cells (VE), and its functions are supported by the surrounding pericytes (P) within the basement membrane (BM), and the end feet of the astrocyte glia (AG). These cellular and non-cellular layers form a compound barrier structure: the neurovascular unit (NVU). Both the vertebrate and invertebrate BBBs

express junctional proteins that form the diffusion barrier (DB), as well as ATP-binding Cassette (ABC) transporters that form the transport barrier and protect the brain from xenobiotics. CG; cortex glia. (B) Substrate predictions for the fly Mdr65 and mouse Mdr1 efflux transporters from substrate docking computer modeling. (C) Homology model of Mdr65 (yellow) overlaid on the mouse Mdr1 template PDB ID: 3G60 (green). Original template ligand, QZ59-RRR, is shown in pink. The enlarged window shows the top-scored pose of ecdysone docked in the Mdr65 model. Also shown are some of the residues predicted to be involved in hydrogen bonding and hydrophobic interactions with the ligand. (D) Competitive *in vivo* efflux transport assay using Rhodamine B and 20E. Fluorescence readings are normalized to wild type (WT) brains injected with Rho B and vehicle. At least 4 biological replicates were performed for each condition. Error bars represent SEM. ANOVA *, $p<0.05$; ***, $p\leq0.001$.

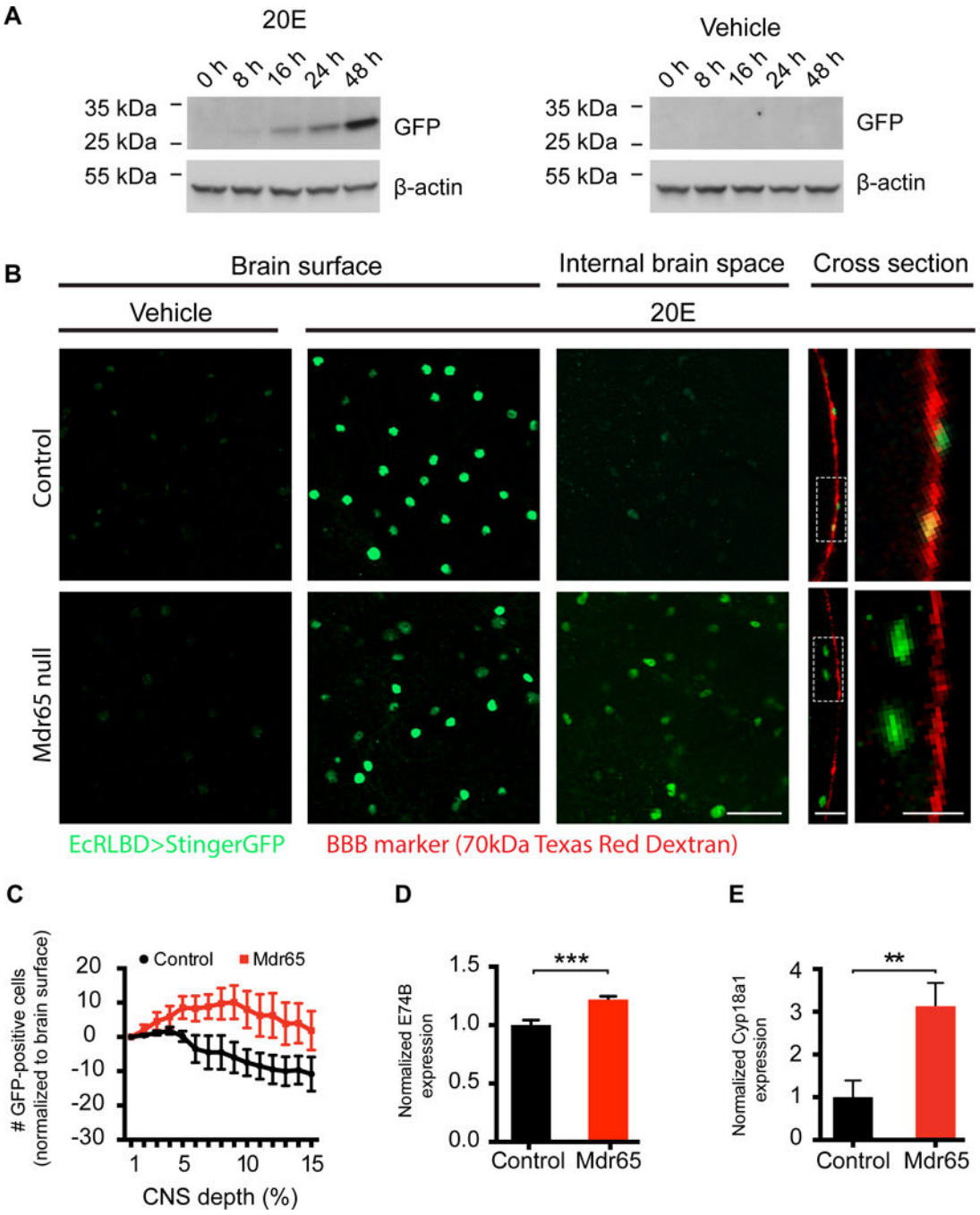

Figure 2. *Drosophila* Mdr65 mutants show altered blood-brain barrier partitioning of 20-hydroxyecdysone

(A) Western blot time-course of EcRLBD>Stinger GFP fly heads following injection of 20E or vehicle. β-actin was used as a loading control. N=2 technical replicates. (B) Confocal images of wild type (i–v) and Mdr65 null mutant (vi–x) brains expressing EcRLBD>Stinger GFP after hemolymph injection of vehicle or 20E. Co-injected 70kDa Texas Red Dextran marks the BBB. Images are shown at the BBB layer (Brain surface; i, ii, vi & vii), below the BBB layer (Internal brain space; iii & viii) and at the optic lobe cross section (Cross section; iv, v, ix & x). Regions from the cross sections were enlarged for clarity (v & x). N> 9

biological replicates. Scale bars, 20 μm (i–iii, vi–viii), 10 μm (iv & ix) and 5 μm (v & x). (C) Quantification of the total number of GFP-positive cells/z-stack section for the initial 15% depth into the optic lobes of EcRLBD>Stinger GFP wild type and Mdr65 null flies hemolymph-injected with 20E. Data were normalized to the number of GFP-positive cells present on the optic lobe surface. N > 5 biological replicates. **(**D & E) QPCR analysis of *E74B* (D) and *Cyp18a1* (E) transcript levels in whole brains from wild type and Mdr65 null flies (without the EcRLBD>Stinger GFP reporter). Error bars represent SEM. T test **, $p<0.005$; ***, $p\leq0.001$.

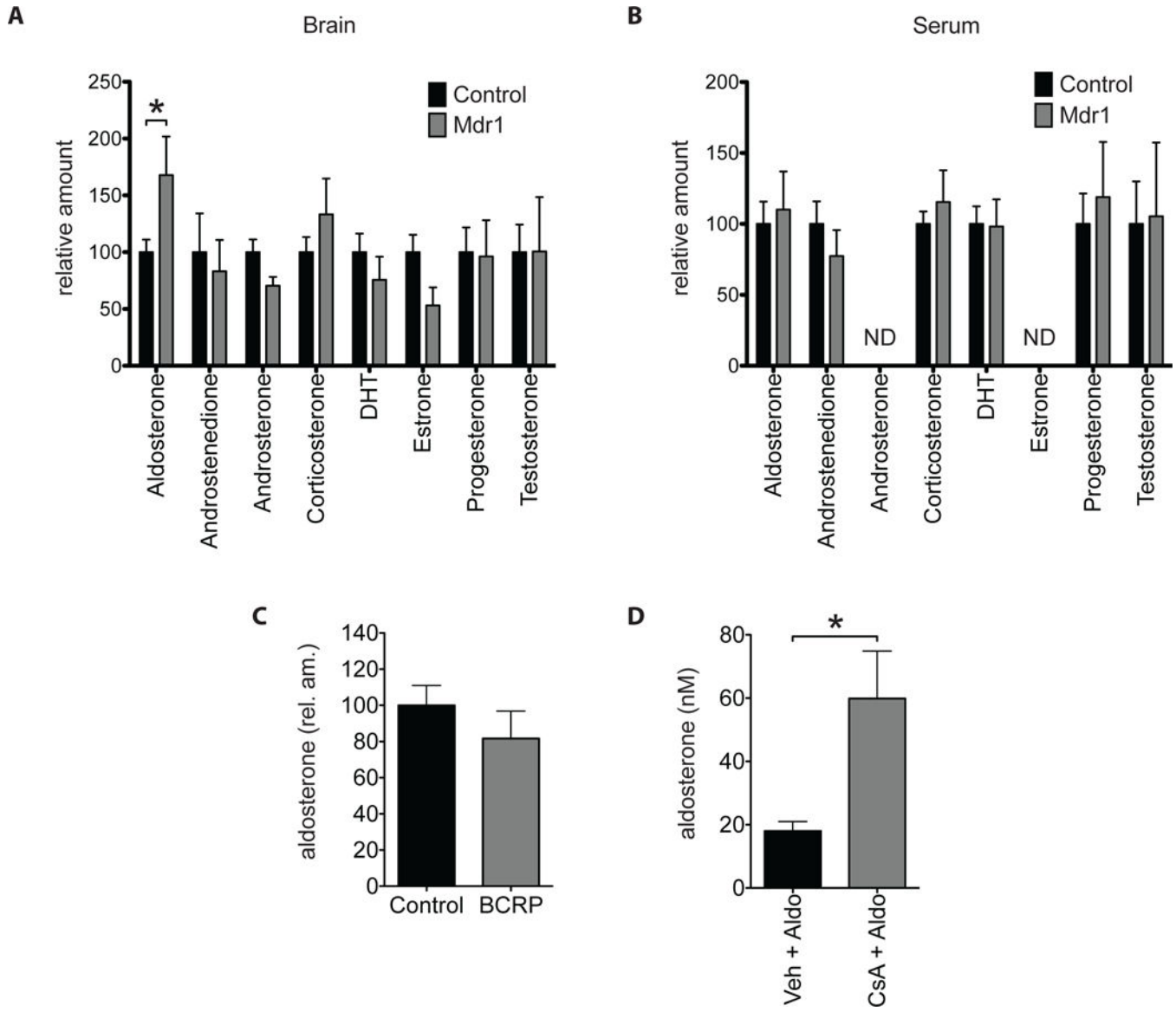

Figure 3. Endogenous aldosterone levels are increased in Mdr1 mutant mice

(A and B) HPLC-MSMS analysis of endogenous steroids from whole brains (A) and sera (B) of adult male Mdr1 control and mutant mice. N= 18 control and 7 Mdr1 mutants. ND, no data. (C) HPLC-MSMS analysis of endogenous aldosterone from whole brains of adult male BCRP control and mutant mice. N=18 Controls and 9 BCRP mutants. (D) HPLC-MSMS analysis of aldosterone from whole brains of wild type mice injected first with either vehicle (n=4) or Cyclosporin A (CsA) (n=4) then followed by aldosterone. Error bars represent SEM. Mann-Whitney test * $p<0.05$.

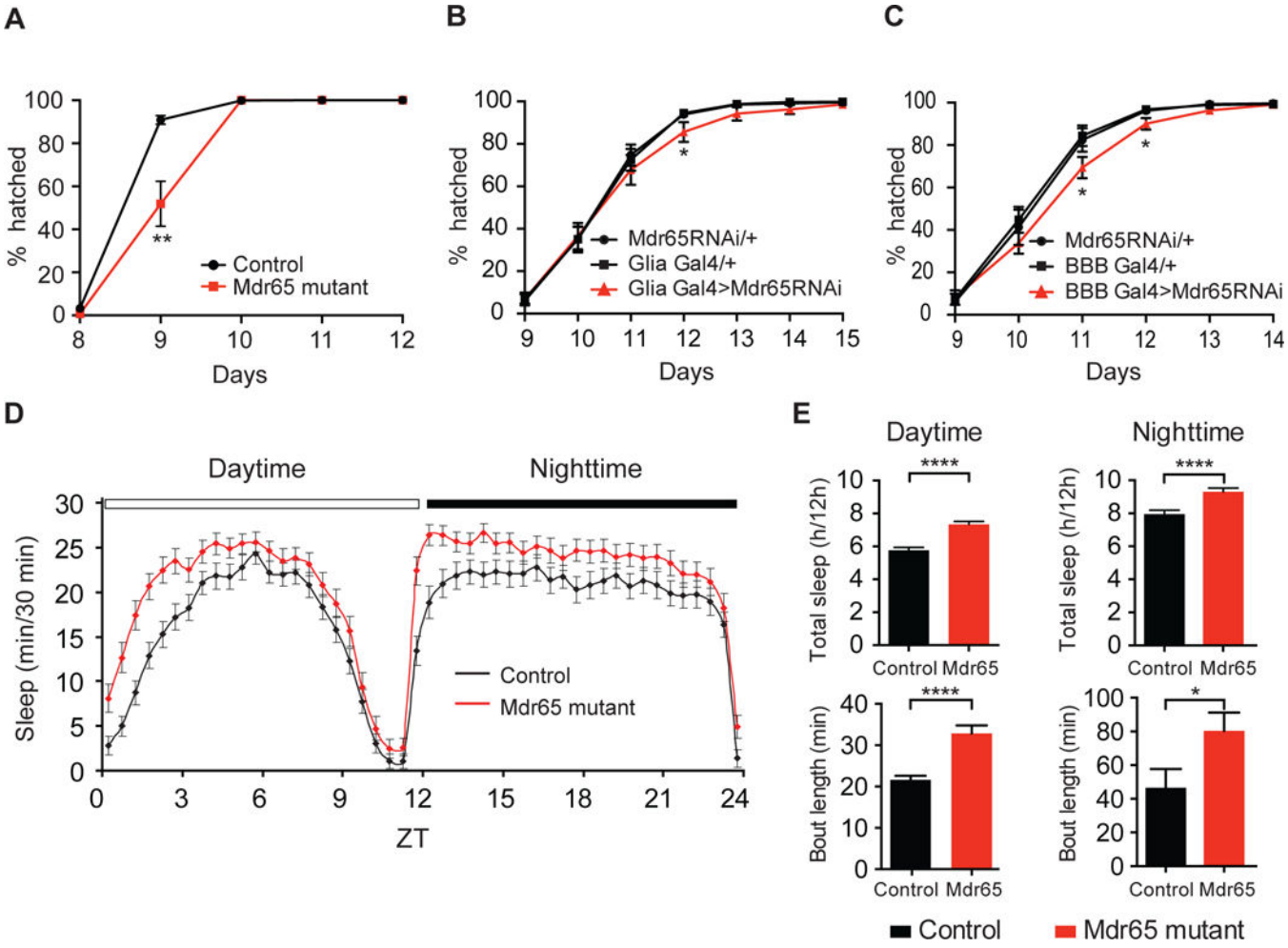

Figure 4. *Drosophila* Mdr65 can modulate behavior

(A–C) The cumulative percentage of adult flies hatching of wild type and Mdr65 null mutants (A), and following knock-down of Mdr65 in all glia (including the BBB) using the driver repo-Gal4 (B; Glia Gal4>Mdr65RNAi) or in the BBB using 9-137-Gal4 (C; BBB Gal4>Mdr65RNAi) compared to the heterozygote transgene controls. *, $p<0.05$; **, $p<0.005$. (D) The length of sleep bouts (min/30 minutes) for wild type and Mdr65 null mutants during the daytime and nighttime. (E) Total amount of sleep (hours/12 hour period) and average bout length during the daytime and nighttime. Error bars represent SEM. T test *, $p<0.05$; ****, $p\leq0.0005$.

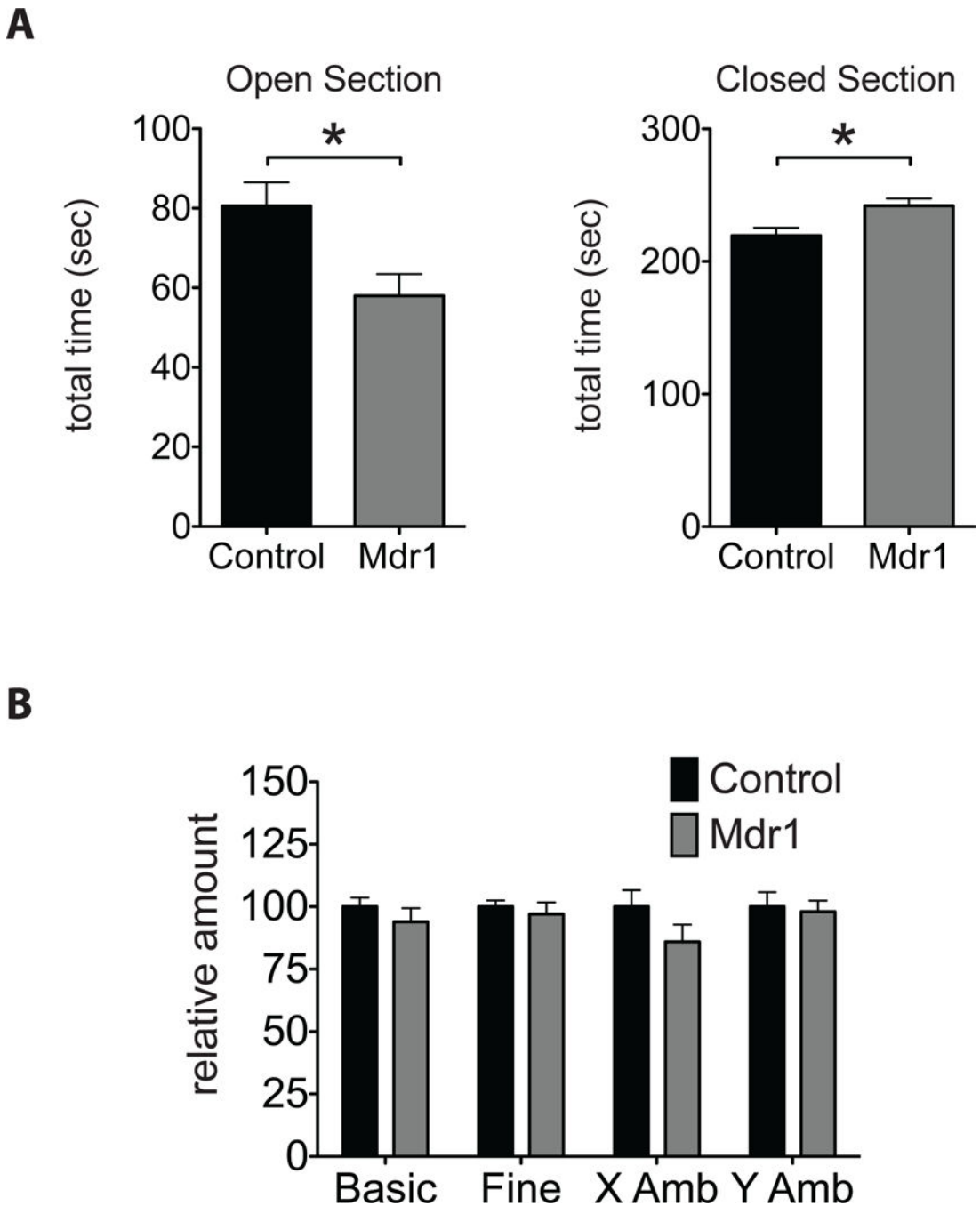

Figure 5. Anxiety-like behaviors are elevated in Mdr1 mutant mice

(A) Amount of time spent in the Open and Closed sections of the elevated zero maze (EZM) apparatus. (B) Amount of movement and ambulation by adult littermate male Mdr1 control and mutant mice during the EZM test. N= 16 controls and 9 Mdr1 mutants. Error bars represent SEM. Mann-Whitney * $p<0.05$.

A

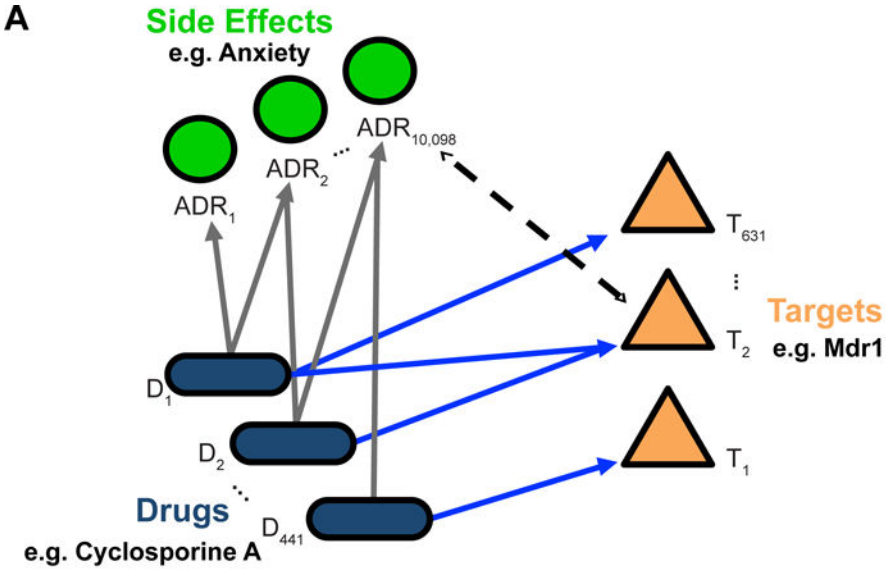

B

Chembl ID	Gene Name	ADR	EF	P-value	Q-value
sp_P41143	OPRD_HUMAN	Anxiety	2.7434	1.98E-17	3.19E-14
sp_P41145	OPRK_HUMAN	Anxiety	2.4041	3.14E-22	5.54E-19
sp_P35372	OPRM_HUMAN	Anxiety	2.1054	1.05E-18	1.75E-15
sp_P31645	SC6A4_HUMAN	Anxiety	2.0792	4.10E-26	7.58E-23
sp_Q01959	SC6A3_HUMAN	Anxiety	1.9879	1.05E-18	1.75E-15
pf_2096682	SCN3A_HUMAN	Anxiety	1.7692	7.70E-12	1.05E-08
sp_P23975	SC6A2_HUMAN	Anxiety	1.7351	2.03E-22	3.59E-19
pf_1907610	ADA1D_HUMAN	Anxiety	1.5486	1.80E-10	2.34E-07
sp_Q12809	KCNH2_HUMAN	Anxiety	1.5351	7.18E-33	1.41E-29
pf_2093864	ADA2A_HUMAN	Anxiety	1.4327	2.25E-15	3.44E-12
sp_P08183	MDR1_HUMAN	Anxiety	1.032	1.64E-09	1.99E-06

C

Chembl ID	Gene Name	ADR	EF	P-value	Q-value
sp_P23975	SC6A2_HUMAN	Emotional Distress	1.5919	4.71E-17	7.37E-14
sp_Q12809	KCNH2_HUMAN	Emotional Distress	1.4862	5.42E-09	6.35E-06
sp_P08183	MDR1_HUMAN	Emotional Distress	1.2774	3.04E-08	3.39E-05

Figure 6. The adverse drug reaction Anxiety is linked with Mdr1-associated drugs

(A) Model diagram for target-ADR enrichment analysis. Enrichment factors were calculated from a unique set of 441 FDA-approved drugs, 10,098 adverse drug reactions (ADRs), and 631 CHEMBL targets after filtering (see Methods). Together, these analyses generated 1,018,208 EFs, of which only 2171 (0.2%) were statistically significant. (B & C) All target-ADR pairs significantly associated with the adverse drug reaction “Anxiety” or “Emotional Distress”. Targets are ordered by enrichment factor (EF) values, with a greater EF value being indicative of an increased number of observed target-ADR associations relative to the

expected number of observations. Q-values indicate degree of confidence that the EF for each target-ADR association is not a false positive.